Final report of OTKA 104477 project
2015.10.30.
Dr. VASS, Csaba

The aims of this project were to introduce, investigate and optimize possible laser-based methods for producing applicable micro- and submicrometer periodical structures (transmission gratings, optical grating couplers, reflection metal grating, polarizer) in transparent and metallic bulk materials and films. The proposed laser-based techniques provide good alternative of ion-etching method for fabrication of submicrometer structures for several applications.

The results can be divided into the following parts:

1. Grating fabrication in UV transparent bulk and thin film targets by LIBWE technique

My preliminary papers report on submicrometer period grating fabrication in bulk fused silica [1-5]. In this project I extended my previous research field: in the first part thin films (Al_2O_3, ZrO_2, Y_2O_3, HfO_2, SiO_2) and other bulk materials (Al_2O_3, fluorides) was structured by two-beam interferometric laser-induced backside wet etching (TWIN-LIBWE).
According to our experiments, the TWIN-LIBWE structuring of sapphire and fluorides did not provides better quality than in case of fused silica targets.

In our first paper supported this OTKA project we reported on producing and characterizing micrometer period surface relief gratings in SiO_2, Al_2O_3, and Y_2O_3 thin films by TWIN-LIBWE technique. To the best of our knowledge, micrometer period grating has not been fabricated into dielectric film by any of the indirect laser-based methods yet – except us.

We determined the optimal etching parameter domain for films has been established for each film with the help of profilometric and atomic force microscopic measurements. Some AFM images of the 1 μm period structures are in the Fig.1 and 2. While the modulation depth and the quality of the etched SiO_2 film is found excellent over a relatively broad fluence (285-600 mJ/cm^2) [4] and pulse quantity (1-150) range, in case of Al_2O_3, and Y_2O_3 films these parameter set is significantly narrower (250-260 mJ/cm^2 and 1-10 pulses, respectively).

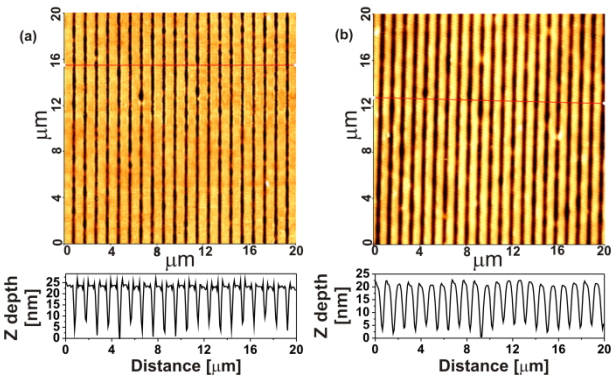

Fig.1. AFM images of gratings (p=1 μm) in Al_2O_3 thin films
(a) film thickness 300 nm, F=260 mJ/cm^2, 3 pulses
(b) film thickness 1000 nm, F=250 mJ/cm^2, 10 pulses

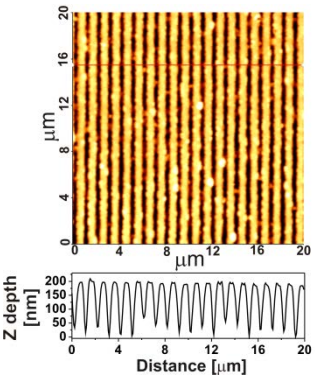

Fig.2. AFM image of grating (p=1 μm) in 200 nm thick Y_2O_3 thin film F=260 mJ/cm^2, 8 pulses

Higher periodicity gratings (p=500 nm) and few hundred nanometers thick films are the most suitable for sensitive OWLS application. For these reason gratings with period around half of micrometer (p=470 nm) were also fabricated in sapphire and yttrium-oxide films (Fig.3.).

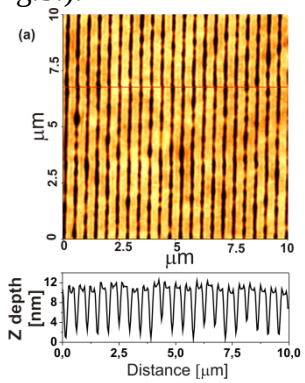

Fig.3. AFM images of grating (p=470 nm) in 300 nm thick Al_2O_3 thin film, F=260 mJ/cm^2, 8 pulses

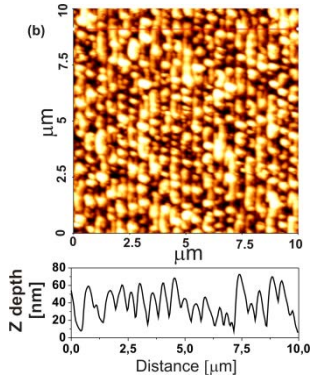

Fig.4. AFM images of grating (p=470 nm) in 200 nm thick Y_2O_3 thin film, F=260 mJ/cm^2, 3 pulses

We have tested the created gratings as waveguide couplers, which prove the suitability of the studied method to produce transmission gratings onto dielectric films. Fig. 5. illustrates two of the grating as successfully incouples the light of He-Ne laser (λ=632,8 nm) into the sapphire and yttrium-oxide film

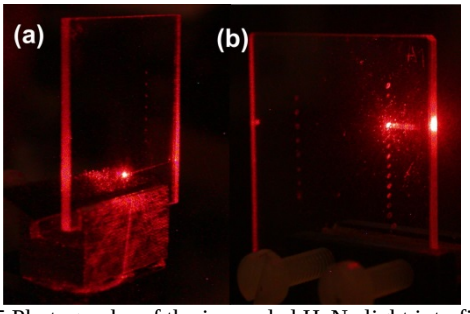

Fig.5.Photography of the incoupled HeNe light into films
(a) 1000 nm Al_2O_3, p=1 µm, MD=16,5nm (avg).
(b) 200 nm Y_2O_3, p=470 nm, MD=15 nm (avg)

It confirms that TWIN-LIBWE made diffraction gratings are suitable for waveguide applications.

A quantitative analysis was carried out to compare and explain the films and structures, which detailed in referred paper [O1].

Referred paper contains these results:

[O1] B. Kiss, F. Ujhelyi, Á. Sipos, B. Farkas, P. Dombi, K. Osvay, **Cs. Vass**, "Microstructuring of Transparent Dielectric Films by TWIN-LIBWE Method for OWLS Applications", JLMN-Journal of Laser Micro/Nanoengineering Vol. 8, No. 3 (2013) 271-275

International conference presentations (1 poster and 1 oral presentation):

Cs. Vass, B. Kiss, F. Ujhelyi, K. Osvay: "Microstructuring of dielectric films by indirect laser etching method for waveguide applications", Fundamentals of Laser Assisted Micro– & Nanotechnologies (FLAMN-13) June 24-28, 2013, St. Petersburg – Russia, poster PS2-23

Cs. Vass, B. Kiss, F. Ujhelyi: "Microstructuring of transparent dielectric films by TWIN-LIBWE method for OWLS applications", The 6th International Congress on Laser Advanced Materials Processing (LAMP2013) July 23–26, 2013., Toki Messe, Niigata, Japan, oral Tu1-OL-11

Hungarian conference presentation (1 poster):

Vass Csaba, Kiss Bálint, Flender Roland, Felházi Zoltán, Ujhelyi Ferenc, Osvay Károly: „Optikai rácsok készítése lézeres eljárásokkal", Kvantumlektronika 2014, Budapest, 2014.11.28. P60 poszter

2. Grating fabrication in transparent materials by ultrashort pulsed laser ablation technique

In the second experiment sequence a Ti:Sapphire-based ultrashort laser system (λ=800 nm; τ_{FWHM}=30 fs, repetition rate: 200 Hz) was used in also two-beam interferometric arrangement. The interfering beams were s-polarized, the incident angle was θ=23.58^o on the front side of target resulted in 1 μm period gratings.

The targets were bulk transparent dielectrics and thin films. Fused silica, sapphire and glass targets were used as bulk target having dimension of 25 mm X 25 mm with thickness of 1 mm. The thin film targets were Al_2O_3, Y_2O_3, HfO_2 and ZrO_2 deposited on fused silica substrates. The morphology of the gratings was studied by a PSIA XE-100 atomic force microscope (AFM) in non-contact mode. Additionally, a Dektak 8 profilometer was applied to help to decide if the grating is solely produced in the dielectric film. We focused only on those structures which etched into the films only, leaving the substrate unmodified under them.

In the femtosecond direct ablation case of fused silica the gratings contain some debris-like formation (Fig. 6), and the groves are not so regular than at nanosecond laser based TWIN-LIBWE arrangement. The grating quality produced in sapphire is good and the modulation depth is 30 nm, which is similar in case of indirect LIBWE method (Fig. 7).

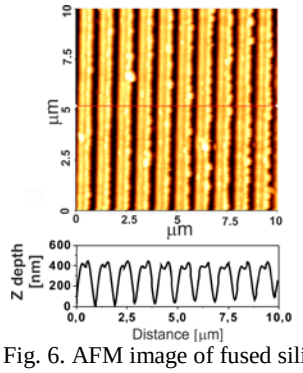

Fig. 6. AFM image of fused silica gratings (770 μJ, 1 pulse)

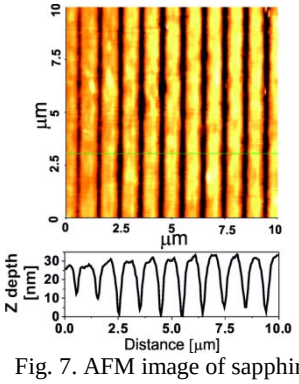

Fig. 7. AFM image of sapphire gratings (600 μJ, 6 pulses)

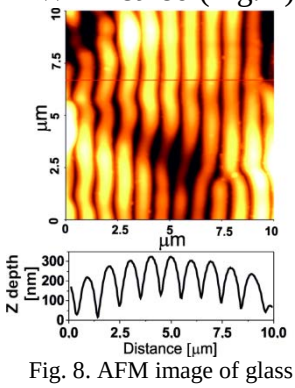

Fig. 8. AFM image of glass grating (600 μJ, 10 pulses)

The quality of glass surface relief grating is rather poor (Fig. 8): the grooves are bended and become irregular, which refer melting and thermal processes could take place during ablation. This effect is similar to previously observed phenomenon in the case of TWIN-LIBWE of fused silica applying high laser fluence and/or high pulse number (see Fig 2. in ref [2]).

In case of transparent films, in the most cases the produced gratings have worse quality applying ultrashort pulse ablation than in case of TWIN-LIBWE structuring (TWIN-LIBWE: Fig. 1-2; ultrashort ablation: Fig. 9-12.). But it is not usual for all materials: ZrO_2

films can be grooved highest quality using ultrashort pulses, than nanosecond indirect ablation (Fig.13.) [O2].

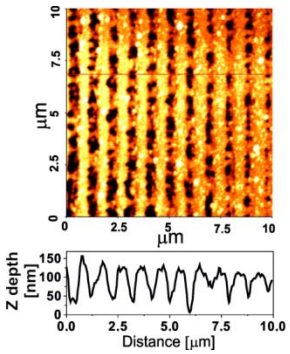

Fig. 9. Al_2O_3 film (300 nm thickness) (600 μJ, 2 pulses)

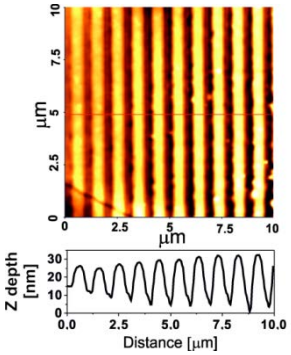

Fig. 10. Al_2O_3 film (1 μm thickness) (600 μJ, 2 pulses)

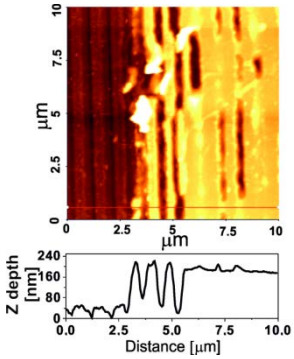

Fig. 11. Y_2O_3 film (200 nm thickness) (600 μJ, 2 pulses)

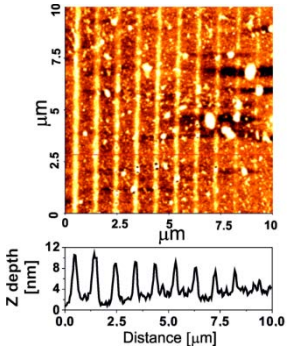

Fig. 12. HfO_2 film (620 nm thickness) (600 μJ, 2 pulses)

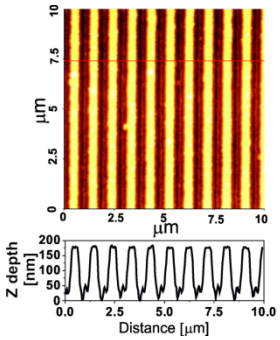

Fig. 13. ZrO_2 film (160 nm thickness) (600 μJ, 1 pulse)

After the fabrication of some hundred grooved spots with both procedures, we have rather certain impressions about the main advantages and difficulties of the two experimental arrangements (TWIN-LIBWE and ultrashort pulse ablation). The most important parameters are summarized in Table 1.

Table 1 Comparison of our two arrangement for microstructuring of transparent materials (TWIN LIBWE versus ultrashort laser-based ablation)

	TWIN-LIBWE	Ultrashort pulse ablation
Laser system	simple (nanosecond)	complicated (femtosecond)
Building up the setup – adjusting equal beam path	relatively simple	difficult
Sample preparation, circumstances	chamber, liquids, chemicals	-
Resolution (determined by the wavelength)	~100 nm	4-500 nm
Processed area (diameter)	≈0.5 mm	<0.1 mm
Optimal number of laser pulses (depends on the target material)	1-100	<10

The final question is obvious: which studied technique is the best method for microstructuring of UV transparent dielectric. According to our results, the answer is not evident: it depends on the aims (e.g. grooved area, required resolution, etc.), on the material, which have to structure, and on the possibilities, infrastructure of the laboratory (available laser, chemicals etc.).

Referred paper contains these results:

[O2] **C. Vass**, B. Kiss, R. Flender, Z. Felházi, P. Lorenz, M. Ehrhardt, K. Zimmer, „Comparative Study on Grating Fabrication in Transparent Materials by TWIN-LIBWE and Ultrashort Pulsed Ablation Techniques", JLMN-Journal of Laser Micro/Nanoengineering Vol. 10, No. 1 (2015), 38-42

International conference presentation (1 oral presentation):

C. Vass, B. Kiss, R. Flender, P. Lorenz, M. Ehrhardt, K. Zimmer, "Micro-structuring of fused silica: nanosecond UV laser in TWIN-LIBWE arrangement versus ultrashort pulse ablation", The 15th International Symposium on Laser Precision Microfabrication (LPM2014), 17-20 June 2014, Vilnius, Lithuania, oral, Tu3-O-8 LPM2014 Program & Technical Digest Page 80

3. Fabrication of micro- and submicrometer period metal reflection gratings by melt-imprint technique

In this sub-task we demonstrated that tin metal gratings can be fabricated by the combination of two simple and cost effective techniques: TWIN-LIBWE and melt-imprint lithography. The master gratings with periods from 3710 to 266 nm were produced in fused silica by TWIN-LIBWE technique. These structures were transferred into bulk tin by melt-imprint technique. The reachable modulation depth of tin replicas was near constant for each period. According to our preliminary measurements, these structures can be applied as reflection grating.

The imprinted tin gratings were produced in two steps. In the first step, surface relief gratings were etched into fused silica plates by two-beam interferometric laser-induced backside wet etching (TWIN-LIBWE) technique based on a Q-switched frequency-quadrupled Nd:YAG laser source. In the second step the grooved fused silica structures were copied into bulk tin. Upon the imprinting both the masters and the pieces of high purity tin were heated up above the melting temperature of Sn by conventional heat source, in ambient air and at normal pressure. After the removal of the oxidized Sn layer the clean, melted tin was placed onto the master's grooved surface. After an approx. 5 minutes cool down period, the resolidified tin with the negative periodic profile of master's imprinted on its surface was removed from the master grating.

The laser fluence and number of pulses were adjusted at each period to cover as high modulation depth range of fused silica master as possible. For an example a photo about a whole tin replica can be seen in Fig. 14 (p=1045 nm).

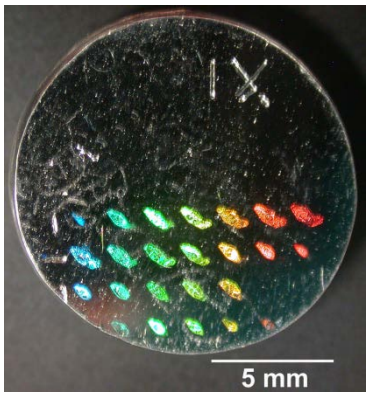

Fig. 14. Photo about a tin replica (p=1045 nm) The parameters of master: constant fluence values in each rows (400-290 mJ/cm^2) and series of pulse number (10-150 pulses)

For examples 2 pairs of AFM images demonstrated the usability of the melt imprinting technique: the quality of resulted metal gratings and theirs replicas is similar (period 2120 nm: Fig. 15; period 266 nm: Fig. 16.). The most important advantage of the introduced technique that nanometers period grating can be fabricated by this method, while other (e.g. direct laser ablation) methods is not suitable to produce such small period structures into metals.

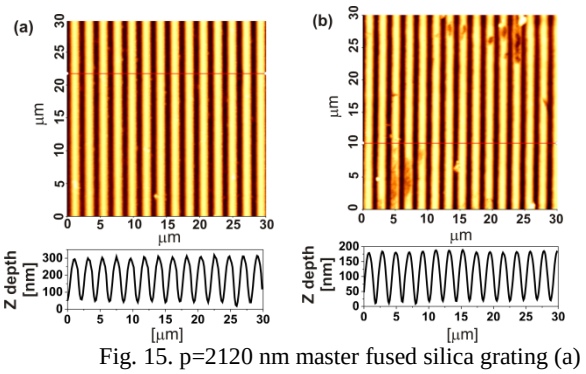

Fig. 15. p=2120 nm master fused silica grating (a) and its tin replica (b)

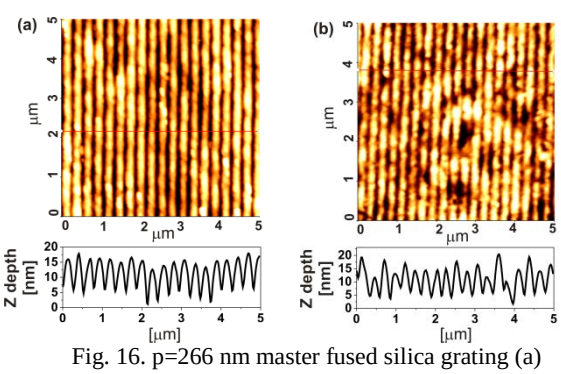

Fig. 16. p=266 nm master fused silica grating (a) and its tin replica (b)

We found during this study that the modulation depths of tin replicas are independent from the modulation depths of master fused silica gratings for each period [O3]. The dependence of average modulation depths of tin structures on the master period was plotted in Fig. 17.: this graph demonstrates the limit of our two-step technique.

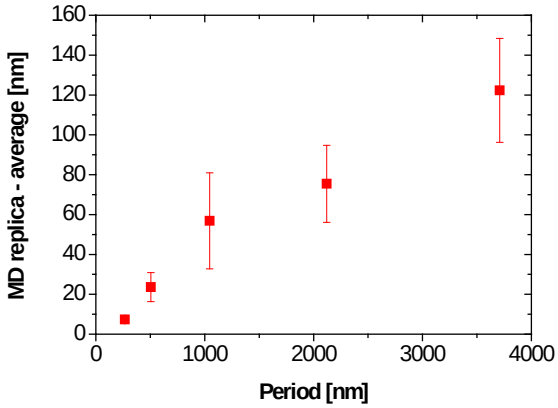

Fig. 17. Average modulation depth of tin replicas vs. grating period

We demonstrated that the fabricated tin replicas can be applied as refection gratings. Photos about the diffracted orders of a HeNe laser beam from the tin replicas can be observed in the Fig.18.

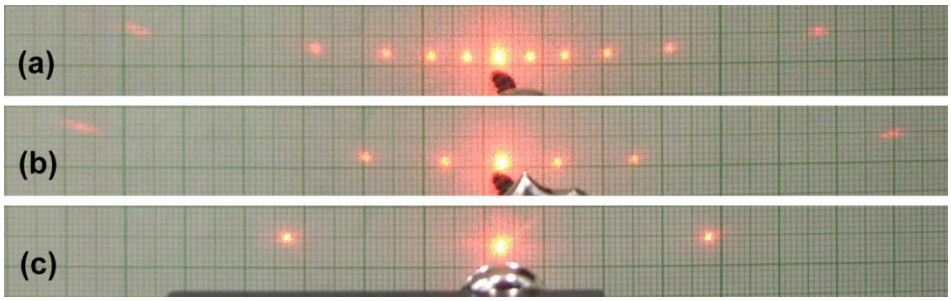

Fig. 18. Photo about the diffracted HeNe spots: (a) p=3710 nm; (b) p=2120 nm; (c) p=1045 nm

Referred paper contains these results:

[O3] B. Kiss, R. Flender, **Cs. Vass**, "Fabrication of Micro- and Submicrometer Period Metal Reflection Gratings by Melt-Imprint Technique", JLMN-Journal of Laser Micro/Nanoengineering Vol. 8, No. 3 (2013) 287-291

International conference presentation (1 poster presentation):

B. Kiss, R. Flender, **Cs. Vass**: "Fabrication of micron and submicron period metal reflection gratings by imprinting technique", The 6th International Congress on Laser Advanced Materials Processing (LAMP2013) July 23–26, 2013., Toki Messe, Niigata, Japan, poster P23

4. Fabrication of polarizer by metal evaporation of fused silica surface relief gratings

Our aim was to produce metal-wire grating polarizers by a simple two-step method. First, fused silica surface relief gratings were generated by two-beam interferometric laser-induced backside wet etching (TWIN-LIBWE) technique. The grating period was varied from 150 nm to 860 nm (p=150, 280, 460, 860 nm) by the changing of the incident angle of interfering beams.

In the second step the gratings were selectively evaporated by thin silver (Ag) film using near grazing incidence (80^o) arrangement to produce narrow metal wires (Fig. 19.). The thickness of metal film was 30±5 nm.

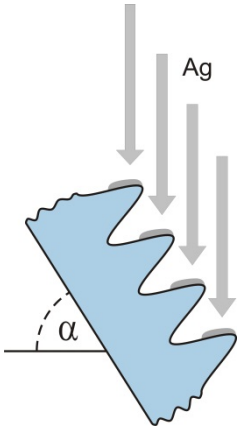

Fig. 19. Scheme of Ag film evaporation onto the grooved surface at near grazing incidence: α=80°, target-gun distance is 30 cm.

The morphology of fabricated metal-wire structures were studied by scanning electron microscopy. Fig. 20 summarizes the surface characteristics of evaporated grooves by increasing grating period and consequently increasing MD. In case of the smallest period of p=150 nm, the grooves are entirely covered by the Ag film (Fig. 20.a), due to the moderate reachable modulation (8-10 nm) of the surface: the grooves do not shield the neighbor ones effectively enough. The 280 nm grating period makes it possible to create structures have higher average MD (20 nm) which supports the formation of periodic Ag structure consist of individual silver lines (Fig. 20b). The uniformity of Ag lines are increasing with the increasing of groove spacing and modulation depth (Fig. 20.c) and found to be the best at p=860 nm (Fig. 20.d).

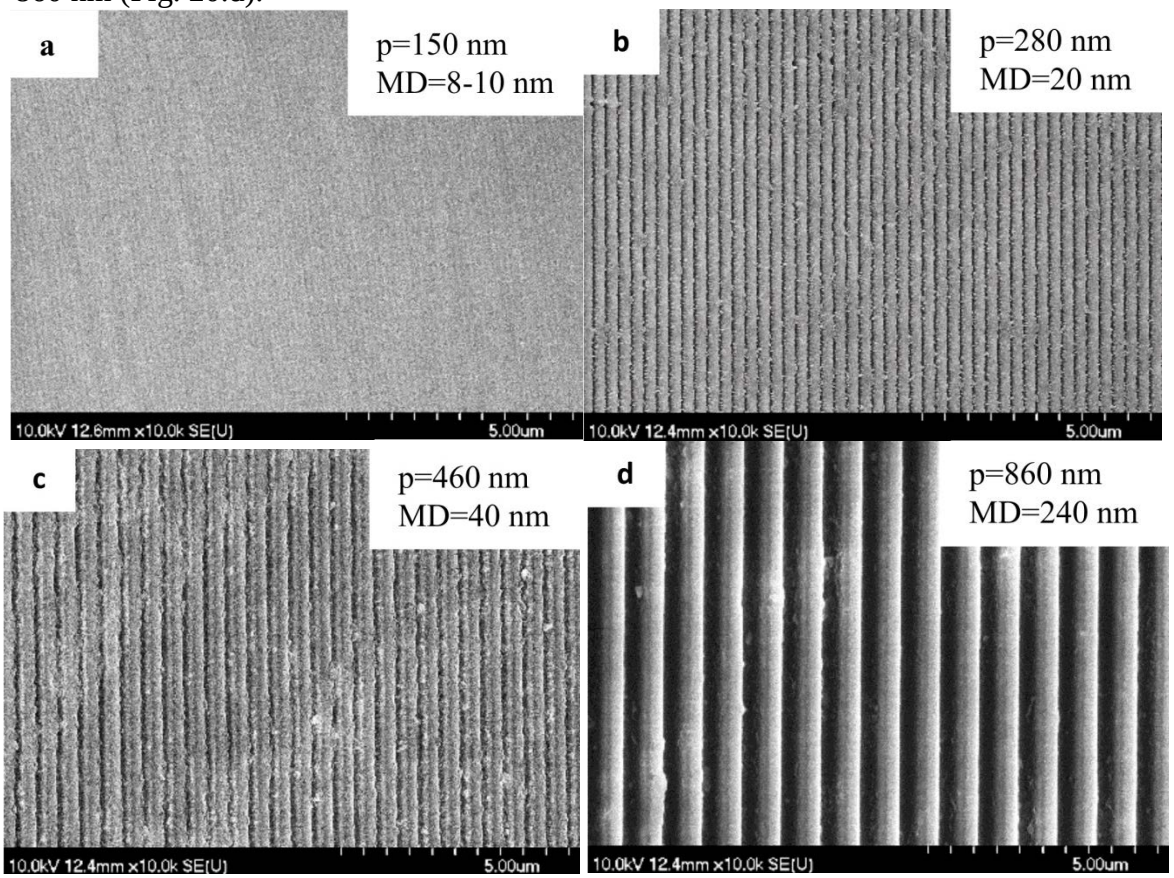

Fig. 20. SEM images of metallic lines created by silver evaporation of gratings.
The inserts show the period and modulation depth of substrate gratings.

The polarizers were tested in infrared wavelength range (λ=1532 nm). According to our measurements, the polarisation contrast of 280 nm period structures was 1:10 for TE:TM transmitted modes. In this case the filling factor of metallic stripes are close to 0.7 [O4].

Referred paper contains these results:

[O4] B. Kiss, R. Flender, J. Kopniczky, F. Ujhelyi, **C. Vass**, “Fabrication of Polarizer by Metal Evaporation of Fused Silica Surface Relief Gratings”, JLMN-Journal of Laser Micro/Nanoengineering Vol. 10, No. 1 (2015) 53-58

International conference presentation (1 poster presentation):

B. Kiss, R. Flender, J. Kopniczky, F. Ujhelyi, **C. Vass**, "Fabrication of Polarizer by Metal Evaporation of Fused Silica Surface Relief Gratings", The 15th International Symposium on Laser Precision Microfabrication (LPM2014), 17-20 June 2014, Vilnius, Lithuania, poster, P53 LPM2014 Program & Technical Digest Page 259

5. Two dimensional numerical modeling of TWIN-LIBWE method for interpretation of submicrometer grating fabrication

The reachable minimum grating period is limited in TWIN-LIBWE by optically: the applied laser wavelength, the incident angle and the relevant refractive indexes determined the achievable minimum grating period. Beside this obvious optical limitation, the thermal effects also limit the achievable resolution. If the heat diffusion length [6] is comparable with the grating constant, the material can be removed not only from the intensity maximums of the interference pattern, but from the minimums, too. This could be the reason that the modulation depth of structure drastically decreased if the period reach the magnitude of the heat diffusion length [4]. However, the heat diffusion length does not describe completely the lateral heat diffusivity. Therefore our motivation was to simulate numerically the grating fabrication during TWIN-LIBWE procedure to verify our above described assumptions. We aimed to study the effects of lateral heat diffusion in this periodical irradiation pattern on the resulted grating structure. To achieve this objective, we extended our previously published one dimensional LIWBE model [7-8] to two dimensional, including the lateral heat diffusion.

Details and conditions of numerical model

The **material removal by LIBWE** procedure can be attributed to:

- thermal (optical) effects (absorption, heat diffusion, change of state)
- chemical effects (modification of hydrocarbon absorber and the carbon contamination of target surface)
- mechanical effects (high pressure jet and bubble) – not included in this model.

2D heat flow equation was solved by the finite differences method.

- Our previous 1D model [7-8] was extended to 2D.

Taking into consideration the followings:

- temperature-dependent thermal parameters of the relevant materials (c(T), k(T))
- melting and vaporization of the relevant materials
- absorption of thin (20-30 nm), carbon contaminated fused silica film
- the removal of boiled layer from the transparent target surface (if the temperature of fused silica layer reaches the boiling point, it will be removed from the surface, and the liquid absorber will flow to its place)

Conditions:

- temporal intensity profile of the laser: Gaussian
- laser intensity profile perpendicular to the grooves: sinusoidal profile
- one grating period was taking into account
- boundary condition: the parameters of elements directly beside the border were mirrored
- heat can propagate both perpendicularly to the liquid-target boundary surface and parallel (perpendicularly the grooves).
- one pulse with average laser fluence: 300-1000 mJ/cm^2
- grating periods: 100-1000 nm
- elementary thickness of one layer (perpendicular to the liquid-target interface): 2.5 nm

- elementary width of an elements (parallel to the liquid-target interface, perpendicular to the grooves): *p*/41 (*p*: period)
- timestep: 1 ps
- optical parameters at 266 nm was approximated by those, which belong to 248 nm
- Pascal code run on an i7-based PC

The profiles of boiled and melted fused silica were calculated for different grating periods (Fig. 21-22.).

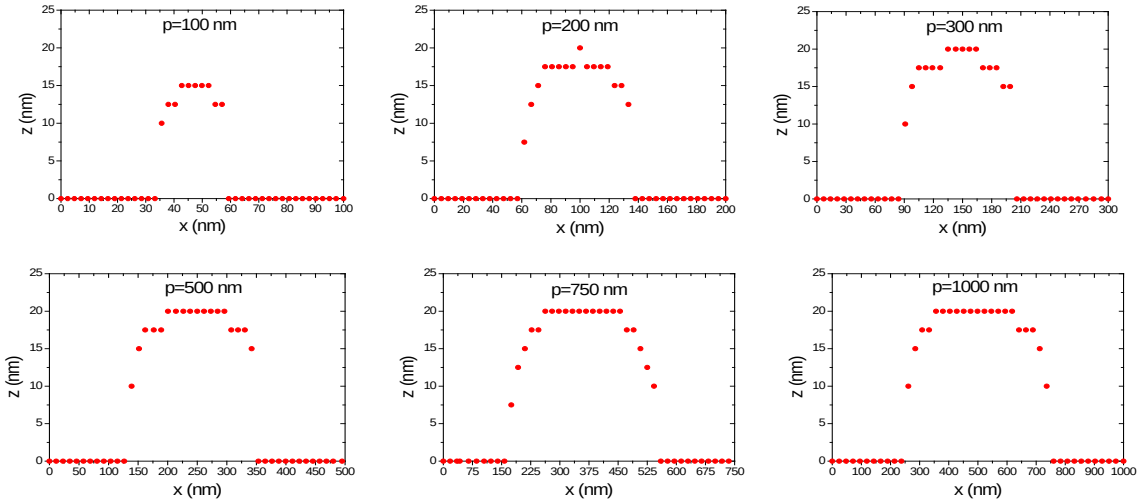

Fig. 21. Calculated boiled profiles of one period grooves (the period is indicated on each graphs)

The calculated width of grooves do not differ significantly at higher (1000 nm) and lower (100 nm) cases: only the modulation depths increased with the increasing of period.

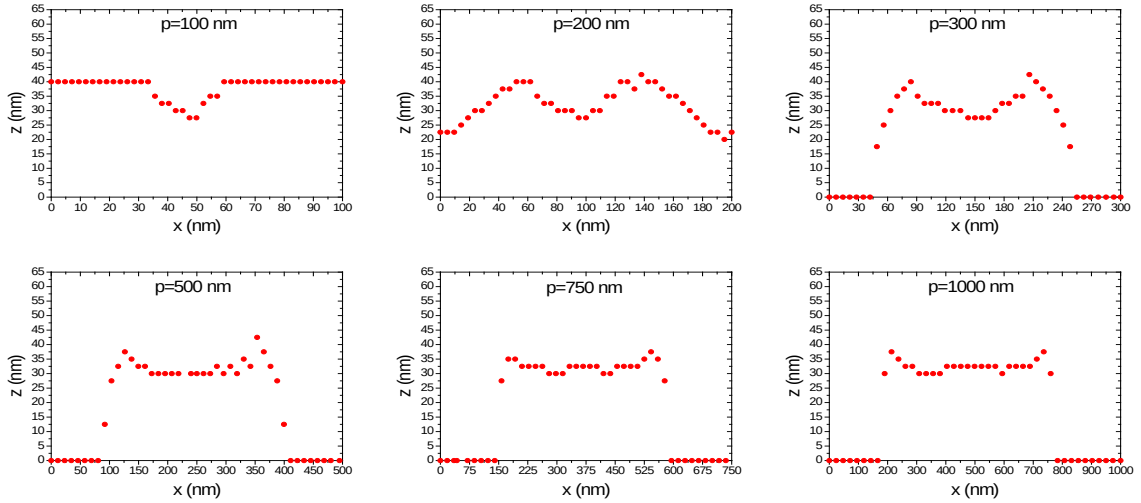

Fig. 22. Calculated melted profiles of one period grooves (the period is indicated on each graphs)

The relative boiled and melted widths of gratings at each period (400 mJ/cm^2) were plotted on graphs in Fig. 23. and 24.

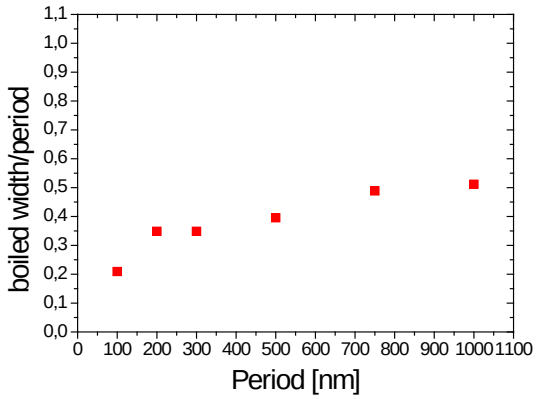

Fig. 23. Relative boiled widths of gratings as a function of grating period (400 mJ/cm^2)

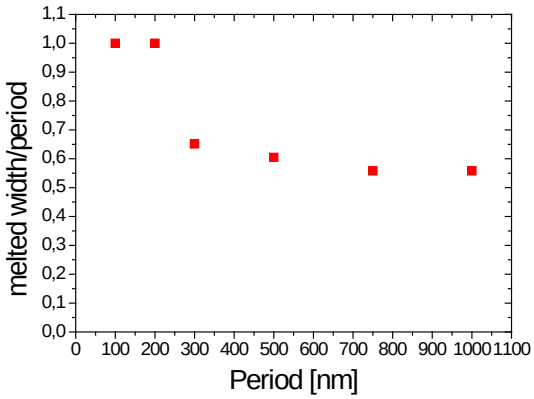

Fig. 24. Relative melted widths of gratings as a function of grating period (400 mJ/cm^2)

We conclude that the calculated modulation depth (boiled depth) is higher for larger period, which means that the lateral heat diffusion become significant at lower grating constant (<300 nm) cases. Furthermore, in the smaller period cases (100-200 nm) grooves melt completely along their whole cross section (in intensity minimums, too) due to the lateral heat diffusion.

The results of our 2D calculations show good agreement with the experimental data [4].

The paper containing these results is under preparing.

International conference presentation (1 poster presentation):

Csaba Vass, Andor Körmöczi, Béla Hopp, „Two dimensional numerical modeling of TWIN-LIBWE method for interpretation of submicrometer grating fabrication in fused silica", COLA 2015, International Conference on Laser Ablation 2015, 31 August – 4 September 2015, Cairns, Australia, Poster Session 1, P003, poster

6. Time-resolved study on grating fabrication in transparent dielectrics

We studied the time evolution of grating structures created into polycarbonate (PC), polymethyl methacrylate (PMMA) and polyimide (PI) by direct laser ablation to understand the relevant phenomena during the laser ablation. The periodic structures were fabricated by a frequency quadrupled nanosecond, Q-switched Nd:YAG pump laser. The spatially filtered, linearly s-polarized UV pulses were steered to the target in two-beam interferometric arrangement, having negligible optical path difference at incident angle of 7.6° and 3°, which corresponds to spatial modulation of ≈1 μm and ≈2,5 μm in the target plane, respectively. The polymer samples were irradiated in the fluence range of 10-800 mJ/cm^2.

The etching setup was completed by an offset-free pump-probe system, which consists of a continuous wave HeNe probe laser (λ=632 nm) and amplified photodiode-oscilloscope system. Special care was taken to get distortion- and background-free monitoring of surface evolution. The CW probe beam illuminated the etching area from the backside of the targets. To separate the effect of phase and amplitude grating, the arising reflected +1st (belongs to the both amplitude and phase grating) and +2nd (corresponds only to the phase grating) diffraction order was monitored by individual photodiodes. Colour filters, prisms and irises were used to realize the undisturbed detection of HeNe intensity: the etching UV photons and the flashing scattered 2nd harmonic of Nd:YAG green pulses were completely filtered.

The rise time of the recorded first and second order signals is ≈3 μs, and this section followed by a relatively constant part (see diagrams on Fig.25.).

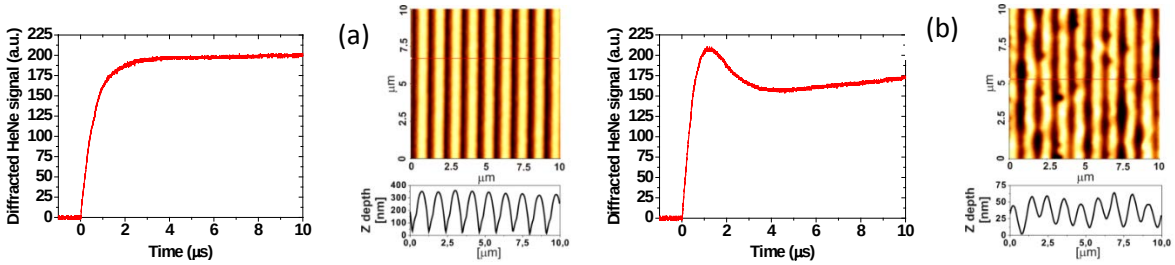

Fig. 25. Detected 1st order signals and AFM images in case of PC. Fluence: 385 mJ/cm^2 (a); 615 mJ/cm^2 (b).

This means that the grooves reach their final depth in the first microseconds: the material removal mostly finishes by 3μs. Moreover, in many cases in first diffraction order a transient peak was observed in the first order diffracted beam 1-2 μs after the ablating pulse (Fig.25.b).

The presence and the parameters of this peak depend on the UV laser fluence and also on the type of the material: this peak is detectable in the low (<170 mJ/cm^2) and high fluence range (>500 mJ/cm^2) at PC, while it can be observed in the whole studied fluence region at PMMA target.

The morphology of the gratings was studied by atomic force microscope (AFM). Melted and resolidified structures were observed on those gratings, where the additional peak was detectable (Fig.25.b). In case of PC the additional peak was not detected in the medium fluence range, while in these cases the grating quality is high, the grooves are perfectly regular.

In case of polyimide, the fluorescence light (accompanying the ablation) overlapped with the transient peak which make difficulties during the data analysis.

However, the transient peak was never observed in the 2nd diffraction order, independently from the UV fluence and type of material. Generally, an amplitude grating does not give rise to diffracted signal in 2nd order. Consequently, the detected 1st order peak can be attributed to a transient amplitude grating, which is due to the different absorption of periodically melted and solid polymer.

On the basis of our experiments the time resolved monitoring of the diffracted signals in the cases of polycarbonate could be a suited method to determine the quality of the ablated gratings, without time consuming ex-situ surface characterization.

Difficulties during this subtask: during the time result studies the TWIN-LIBWE procedure could not be followed by the planned setup, due to the arisen technical problems. Following the principle of gradience we started our studies with small modification: interferometric direct ablation of gratings was studied instead of the TWIN-LIBWE etching, and so the technical difficulties could be eliminated.

The paper containing these results is under preparing.

International conference presentations (2 oral and 1 poster presentations):

B. Kiss, R. Flender, **Cs. Vass**, K. Osvay, “Time-resolved study on grating formation in polycarbonate”, Developments in Optics and Communications / Laserlab III Training School, Riga, Latvia, 9-12 April 2014; poster, P44

C. Vass, R. Flender, B. Kiss, K. Osvay, "Time-Resolved Study on Grating Fabrication in Transparent Dielectrics", The 15th International Symposium on Laser Precision Microfabrication (LPM2014), 17-20 June 2014, Vilnius, Lithuania, oral, Tu3-O-4 LPM2014 Program & Technical Digest Page 76

Csaba Vass, Roland Flender, Balint Kiss, Karoly Osvay, „Time-resolved study on periodic microstructure fabrication in polymers", COLA 2015, International Conference on Laser Ablation 2015, 31 August – 4 September 2015, Cairns, Australia, Session 10, O-46; oral

Hungarian conference presentation (1 poster):

Flender Roland, **Vass Csaba**, Kiss Bálint, Osvay Károly: „Polimerekbe készített optikai rácsok kialakulásának időbontott vizsgálata" Kvantumlektronika 2014, Budapest, 2014.11.28. P34 poszter

References

[1] C. Vass, K. Osvay, B. Hopp, Z. Bor: "104 nm period grating fabrication in fused silica by immersion two-beam interferometric laser induced backside wet etching technique", Appl. Phys. A 87 (2007) 611-613

[2] C. Vass, K. Osvay, M. Csete, B. Hopp: "Fabrication of 550 nm gratings in fused silica by laser induced backside wet etching technique", Appl. Surf. Sci. 253 (2007) 8059-8063

[3] C. Vass, K. Osvay, B. Hopp: "Fabrication of 150 nm period grating in fused silica by two-beam interferometric laser induced backside wet etching method", Opt. Express 14 (2006) 8354-8359

[4] C. Vass,·K. Osvay, T. Véső, B. Hopp, Z. Bor: "Submicrometer grating fabrication in fused silica by interferometric laser-induced backside wet etching technique", Appl. Phys. A 93 (2008) 69–73

[5] B. Kiss, Cs. Vass, P. Heck, P. Dombi, K. Osvay: „Fabrication and analysis of transmission gratings produced by the indirect laser etching technique", J. Phys. D: Appl. Phys. 44 (2011) 415103 (5pp)

[6] D. Bäuerle, Laser Processing and Chemistry, 3rd edn. (Springer, Berlin, 2000)

[7] Cs. Vass, B. Hopp, T. Smausz, F. Ignácz, "Experiments and numerical calculations for the interpretation of the backside wet etching of fused silica", Thin Solid Films 453-454 121-126 (2004)

[8] Cs. Vass, J. Budai, Z. Schay, B. Hopp, "Interpretation and Modeling of Laser-Induced Backside Wet Etching Procedure", JLMN-Journal of Laser Micro/Nanoengineering 5(1) 43-47 (2010)